Journal of Magnetism and Magnetic Materials 427 (2017) 168–174

Contents lists available at ScienceDirect

Journal of Magnetism and Magnetic Materials

journal homepage: www.elsevier.com/locate/jmmm

Improvement of drug delivery by hyperthermia treatment using magnetic cubic cobalt ferrite nanoparticles

Chaitali Dey[a,*], Kaushik Baishya[b], Arup Ghosh[b,c], Madhuri Mandal Goswami[b,**], Ajay Ghosh[d], Kalyan Mandal[b]

[a] Centre for Research in Nanoscience & Nanotechnology, Block-JD-2, Sector-III, Salt Lake, Kolkata 700106, India
[b] S.N. Bose National Centre for Basic Sciences, Block-JD, Sector-III, Salt Lake, Kolkata 700106, India
[c] Department of Physics, Indian Institute of Science Education and Research (IISER) Pune, Dr. Homi Bhabha Road, Pashan, Pune 411008, India
[d] Dept. of Applied Optics and Photonics, University of Calcutta, Block-JD-2, Sector-III, Salt Lake, Kolkata 700106, India

ARTICLE INFO

Keywords:
Magnetic nanoparticles
Cobalt ferrite
Magnetic hyperthermia
Drug release

ABSTRACT

In this study, we report a novel synthesis method, characterization and application of a new class of ferromagnetic cubic cobalt ferrite magnetic nanoparticles (MNPs) for hyperthermia therapy and temperature triggered drug release. The MNPs are characterized by XRD, TEM, FESEM, AC magnetic hysteresis and VSM. These MNPs were coated with folic acid and loaded with an anticancer drug. The drug release studies were done at two different temperatures (37 °C and 44 °C) with progress of time. It was found that higher release of drug took place at elevated temperature (44 °C). We have developed a temperature sensitive drug delivery system which releases the heat sensitive drug selectively as the particles are heated up under AC magnetic field and controlled release is possible by changing the external AC magnetic field.

1. Introduction

In recent years, studies on nanomaterials have drawn immense attention for their high surface to volume ratio and high porosity which make them efficient absorber and can be used in the field of nano-carriers especially in case of drug delivery vehicles [1–4]. Therefore proper design of smart nano-carrier for drug delivery is a very challenging task to make the drugs to be loaded efficiently [5] and delivered to proper region of interest in the body [2]. In this regard an ideal nano-carrier system should have several suitable properties such as biocompatibility, water solubility, small size for effective cellular uptake and safe excretion from the biological system after functioning [6,7]. Improved cellular uptake of many nano-carrier systems has been claimed in several studies [1,2,8]. People have designed few nano-carriers in which the drug molecules can be loaded efficiently, but some time remaining of drugs inside them become less, as most of the drugs are removed during the carrier surface is made hydrophilic for easy cellular uptake. Elimination of the drug carriers from the biological system after carrying out their diagnostic or therapeutic functions is another important aspect to consider [9]. Though these works have their own importance, nevertheless, this task still remains challenging in most of the nano-carrier systems. Hence, if it is possible to make a good biocompatible and stable nano particle with high cellular uptake which can display some important characteristics in the field of drug delivery by some triggered drug release way, such as heat, may open the new vistas of drug release methodology by using nanoparticles [2,10–12].

If such nano-carriers are magnetic in nature then they can be able to serve both as drug carrier and good drug delivery agent as well by magnetically triggered way [3,13–17]. Release of drug from such material can also be monitored by magnetically induced heat treatment methodology. It is known that if magnetic particles are kept under alternating current (AC) magnetic field, they are heated up due to the core loss in such nanoparticles and transforms magnetic energy into heat [14,18,19]. The heat generated by this method may be utilized to destroy cancer cells in one hand and on the other, can be applied to release drugs from magnetic particles after delivery of the drug loaded particles to the tumor region. In this treatment the AC magnetic field of different range of frequency may also be applied to control the heating effect in the range of 41–45 °C for the magnetic nanoparticles placed in the body as this temperature is ideal to kill cancer cells but keep the normal cells alive [20]. But there are many limitations in use of such magnetic particles such as very poor heating efficiency, internalization of particles with cells, stability, biocompatibility etc. [21]. Major efforts

* Corresponding author.
** Corresponding author.
E-mail addresses: chaitalidey29@gmail.com (C. Dey), madhuri@bose.res.in (M.M. Goswami).

http://dx.doi.org/10.1016/j.jmmm.2016.11.024
Received 26 June 2016; Received in revised form 3 November 2016; Accepted 5 November 2016
Available online 08 November 2016
0304-8853/

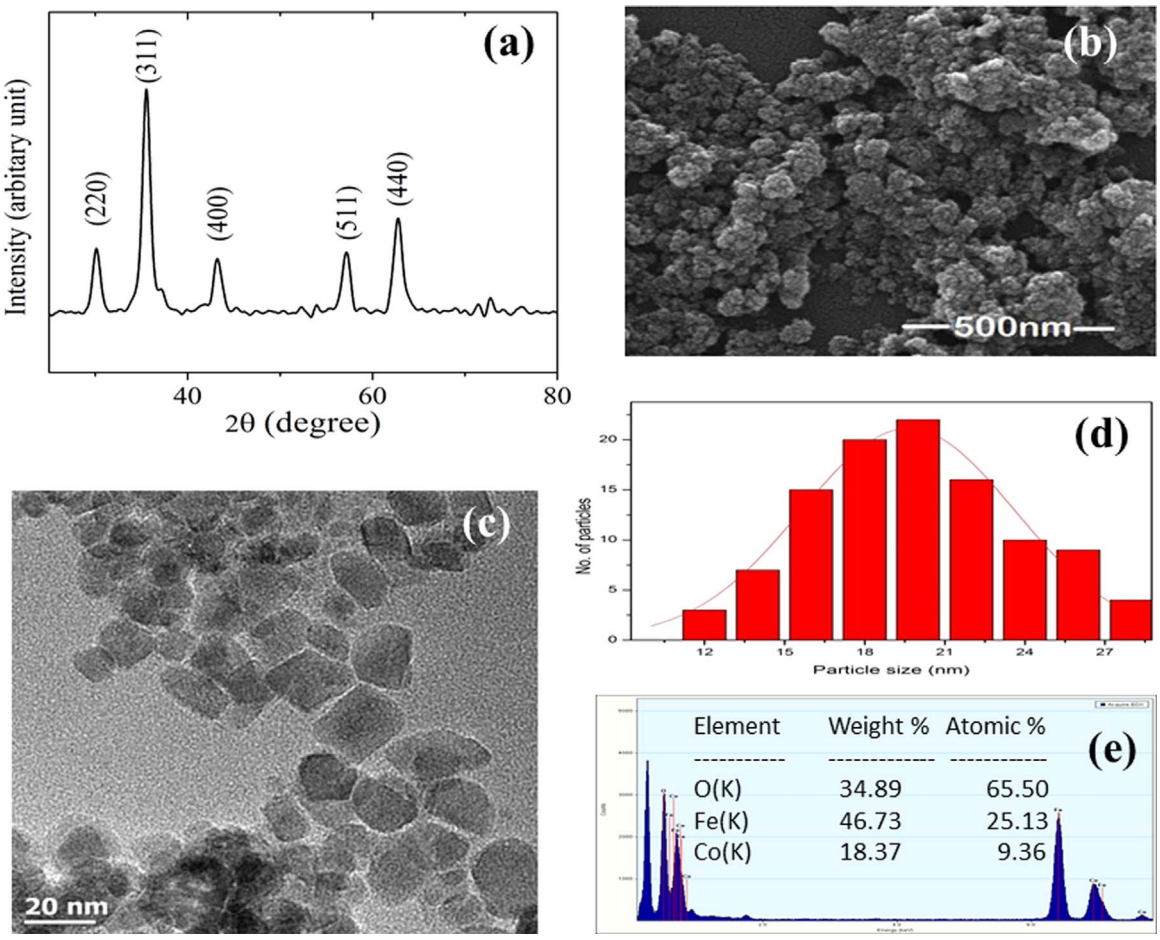

Fig. 1. (a) Room temperature X-ray diffraction pattern, (b) FESEM micrograph of $CoFe_2O_4$ NPs, (c) TEM image of $CoFe_2O_4$ and (d) the size distribution histogram of $CoFe_2O_4$ MNPs. (e) EDAX spectra of $CoFe_2O_4$ MNPs.

should therefore be given to optimize such nanoparticles' heating efficiency, by tuning some of the key parameters such as size, shape, magnetic anisotropy, saturation magnetization of the nanoparticles, internalization of the particles with the cells, etc. The usability of iron oxide nanoparticles in this regard is quite higher [8,17,22] as iron and their oxides can be metabolized and transported by proteins and it also has the most successful result in the area of nano-medicines [22,23]. These materials have already been suggested for the use in hyperthermia by applying an AC magnetic field [18]. But, cobalt-iron oxide has not been tested in this field. As cobalt and iron both exist in human body, it would be very interesting to know if it is fruitful in hyperthermia or not. The special advantages of cobalt ferrite MNPs are that their stability is quite higher as Co in +2 state and Fe in +3 state is very stable and aerial oxidation generally does not take place in such materials.

In order to overcome some of limitations, we have synthesized $CoFe_2O_4$ nano-cubes and studied their detail AC and DC magnetic properties for the promising hyperthermia treatment and drug delivery applications. Doxorubicin (DOX), a traditional anticancer drug from anthracycline family, which is used to cure a wide range of cancers [24]. However it has serious adverse side effects. Therefore use of such drugs in a low quantity with increase of its efficiency with the help of magnetic hyperthermia is also very challenging job.

2. Experimental details

2.1. Synthesis of particles

The precursor salts ferric chloride ($FeCl_3$, $6H_2O$) and cobalt chloride ($CoCl_2{\cdot}4H_2O$), ethylene glycol, ethanol, Urea, Triton X-100, oleylamine etc. were procured from Sigma-Aldrich. In a typical synthesis of $CoFe_2O_4$ NPs, 3.24 g of $FeCl_3$, $6H_2O$ and 1.4 g of $CoCl_2$, $4H_2O$ were dissolved well in 70 ml ethylene glycol. To make the medium basic, 10 g of Urea in 70 ml ethanol was added to the solution and stirred vigorously at 100 °c temperature until a homogenous solution was obtained. After about 1 h, the solution turned into dark brownish when 2 ml oleylamine and 2 ml Triton X-100 was added to the solution and the stirring continued for the next 6 h along with continuous heating. After 6 h, the solution was allowed to cool. The volume of the solution was made doubled by adding ethanol and kept overnight. Afterwards, the solution was centrifuged and particles were obtained thereafter by washing with deionized water, ethanol and acetone. After drying, the particles were ground well in a mortar and annealed at 300 °C for 1 h before further characterizations were done.

2.2. Physical properties measurements

The phase and crystallinity of such synthesized MNPs were first characterized by X-ray diffraction (XRD) patterns measured at room temperature taken in a Rigaku Miniflex II X-ray diffractometer using Cu-K_α (λ=0.154 nm) radiation under a 2θ range of 20–80°. The surface morphology was studied in a field emission scanning electron microscope (FESEM, FEI Quanta-200) at 20 kV and in a transmission electron microscope (TECHNAI G2 SF20 ST TEM) at 200 kV. JASCO FTIR-6300 was used for the confirmation of interaction between folic acid and sample. The DC magnetic field dependent properties of the MNPs were measured in a vibrating sample magnetometer (VSM, Lake Shore Model-7144) under 300 Oe external field from 80 K to 300 K.

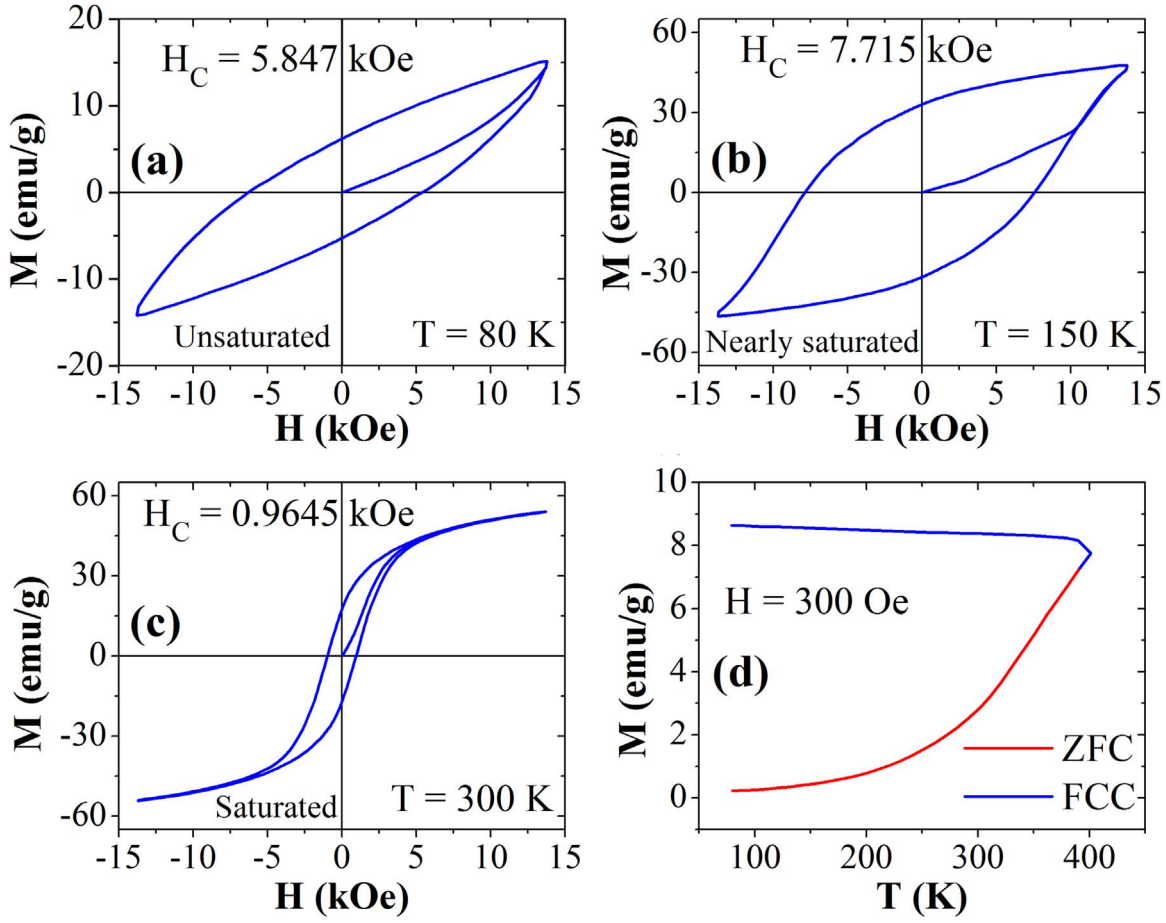

Fig. 2. DC Magnetic hysteresis loops of $CoFe_2O_4$ NPs at (a) 80 K, (b) 150 K and (c) 300 K. (d) Temperature dependent magnetization of $CoFe_2O_4$ NPs.

The room temperature AC magnetic field dependent measurements were carried out in our laboratory made AC hysteresis measurement setup with very basic circuit [19].

2.3. Folic acid coating and drug loading

The cobalt ferrite MNPs were coated with folic acid (FA) which was purchased from Sigma Aldrich having purity of 97%. For FA coating first 10 mg of FA was taken in 10 ml of distilled water and shaken well. Then 10 mg of particles were dispersed in this FA solution and the mixture was stirred overnight in dark. Then the FA coated particles were separated from solution by magnetic separation method to remove excess FA which are unbound to particles and washed well for several times by water and dried overnight. Then this FA functionalized particles were subjected for FT-IR study to check the coating of particles by FA. The size of the particle before and after FA coating was measured by dynamic light scattering (DLS) experiments on a Malvern Zetasizer Nano-S instrument at 25 °C to ensure the folic acid coating.

For drug loading, 10 mg of FA coated $CoFe_2O_4$ NPs were taken in 5 ml of water and to this 100 μL of sodium hydroxide (1×10^{-3} M) was added to make the particles water soluble. The doxorubicin hydrochloride (Dox), purchased from Sigma Aldrich having purity of 98–102%, was dissolved in de-ionized water with concentration of the solution 6.897×10^{-4}M. 100 μL of this Dox solution was added to the above particles and allowed to stir for 1 h. Then these particles are separated from solution and were gently washed with pH 7.4 PBS buffer and again dried and loading efficiency was checked with the help of UV–vis absorption spectra taken before and after loading the drug.

3. Results and discussion

3.1. Structural and morphological analysis

Fig. 1(a) depicts the XRD patterns for the synthesized $CoFe_2O_4$ MNPs. All the diffraction peaks matches with the JCPDS (card no. 22–1086) of $CoFe_2O_4$ MNPs. The crystalline size of the sample is 10.5 nm using the (311) peak, estimated using Scherrer's equation [25]. The FESEM image of the synthesized $CoFe_2O_4$ NPs is shown in Fig. 1(b). The individual MNPs are not visible from Fig. 1(b) due to the smaller size of them and low resolution of the instrument. Therefore, the TEM image has been taken and given in Fig. 1(c) which confirms the cubic shape of the NPs. To know about the size distribution, a distribution histogram is presented in Fig. 1(d) which has been prepared after investigating several SEM and TEM images. The NPs have an average size of 19.6 ± 0.27 nm. Fig. 1(e) represents the energy dispersive spectra (EDAX) of the cobalt ferrite MNPs. The atomic percentage of the constituent elements is given in the inset of Fig. 1(e) which indicates the presence of Co, Fe, and O. Though these are the elements present in Co-ferrite but stoichiometrically do not meet the exact value. It may be because 'O' is lighter and non metallic element and in most of the cases such elemental analysis does not meet the expected value. But XRD analysis proves formation of $CoFe_2O_4$.

3.2. DC Magnetic characterization of $CoFe_2O_4$ nanoparticles

In order to study the static magnetic response of $CoFe_2O_4$ MNPs, the field dependent DC magnetization (M-H curves) of $CoFe_2O_4$ nanostructures at 80 K, 150 K and 300 K has been measured and represented in Fig. 2(a), (b) and (c) respectively. The hysteresis loop at

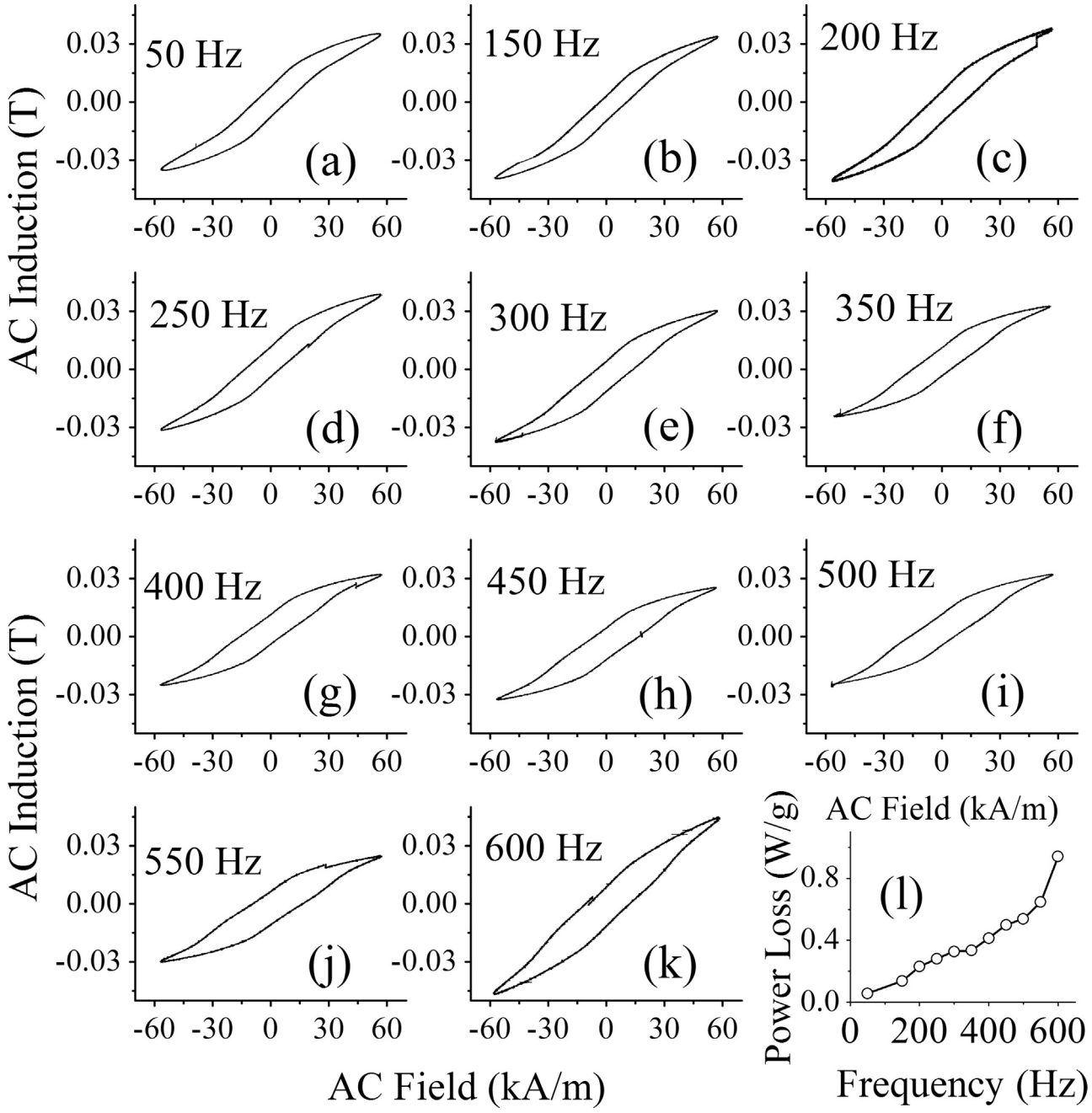

Fig. 3. (a-k) Room temperature AC magnetic hysteresis loops for $CoFe_2O_4$ MNPs in the frequency ranges from 50 Hz to 600 Hz. (l) Frequency dependent power loss in $CoFe_2O_4$ MNPs.

80 K is not saturated and this is why its coercivity (H_C) is smaller compared to as of the 150 K hysteresis loop. It can be observed from the figures that the H_C of the MNPs decreases with the increase in the measurement temperature, which can be understood by considering the influence of thermal fluctuations of the blocked moment across the anisotropy barrier. It suggests that the anisotropy of the system decreases with increasing temperature. As the temperature increases, the thermal agitation starts to weaken the anisotropy barriers and this in turn diminishes the H_C significantly. The value of the saturation magnetization of our MNPs is comparable to the other reported cobalt ferrite MNPs [26,27]. The value is ~54 emu/g at 300 K. We have observed that the values are smaller as compared to the bulk value (80.8 emu/g) for $CoFe_2O_4$ [27]. The smaller value of saturation magnetization of the MNPs as compared to the bulk materials may be due to the surface effect.

The zero field cooled (ZFC) and field cooled cooling (FCC) temperature dependent magnetization of $CoFe_2O_4$ NPs in presence of 300 Oe field is plotted in Fig. 2(d). The ZFC M-T curve shows a monotonic increase in the magnetization with increasing the temperatures between 200 K and 400 K. In the lower temperatures, the freezing of moments occurs due to the crystalline anisotropy and defects. As the temperature increases, the increased thermal energy helps the moments to align along the applied magnetic field. While the FCC M-T curve shows the usual temperature dependent nature of magnetization. Our $CoFe_2O_4$ NPs seems to have a blocking temperature above 400 K. Therefore, up to 300 K, our system remains in the ferromagnetic regime.

3.3. AC magnetic properties

The room temperature (300 K) AC magnetic hysteresis loops of $CoFe_2O_4$ NPs were measured within the frequency range from 50 Hz to

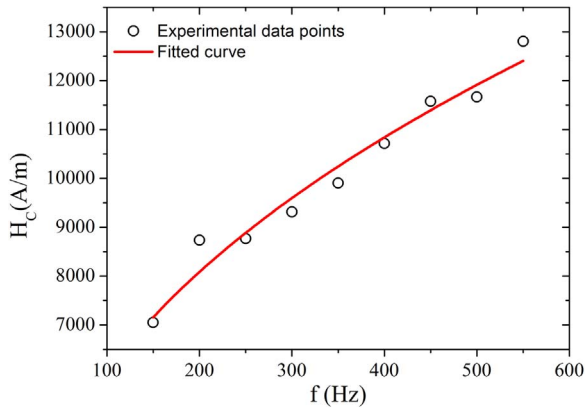

Fig. 4. Experimental (open circles) and fitted (solid line) Frequency dependent coercivity for $CoFe_2O_4$ NPs.

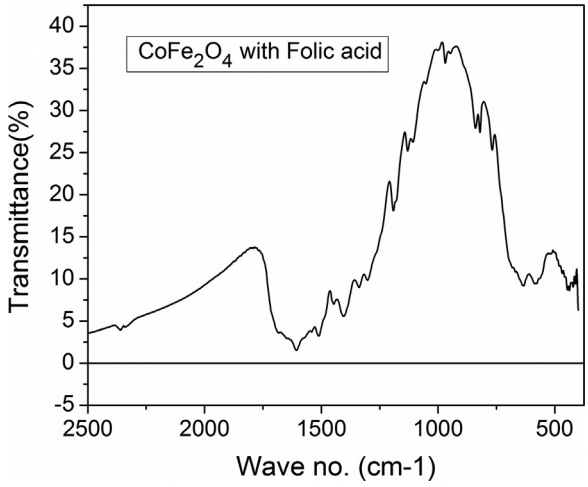

Fig. 5. FT-IR spectra of folic acid coated magnetic cobalt ferrite nanoparticle.

600 Hz and shown in Fig. 3. The maximum field was kept below 60 kA/m and produced by the primary AC coil through series LCR resonant circuit. H_C of the MNPs increases with increasing the field frequency, which in turn enhances the area under the hysteresis loops. The variation of H_C can be explained in terms of breaking of domains with increasing frequency which results in an increase in the total number of active domain walls that take part in the dynamic reversal process of the sample's magnetization. Larger the number of domain, more the energy is required to rotate them altogether. This actually causes an

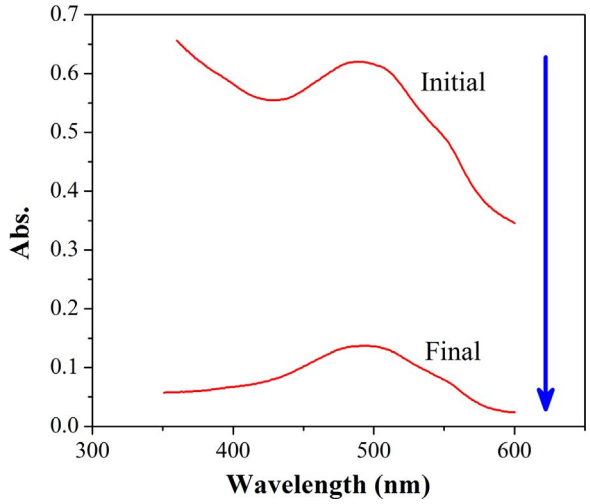

Fig. 7. UV–visible spectra of initial drug solution and finally after drug loading by the particles.

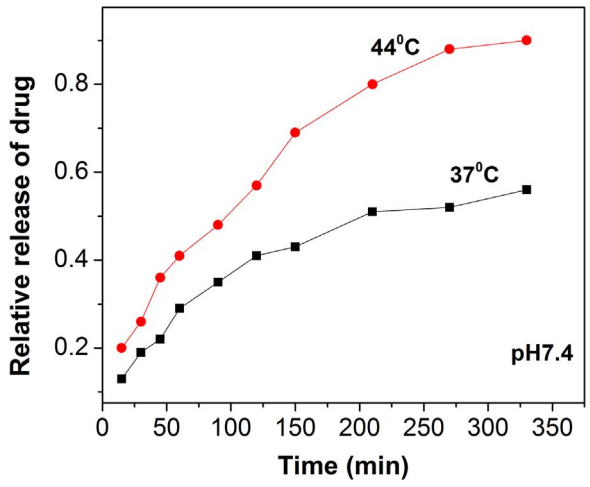

Fig. 8. Time dependent drug release graphs of DOX loaded $CoFe_2O_4$ NPs in PBS solution at two different temperatures.

increase in phase lag between the applied AC magnetic field and the sample's instantaneous magnetization. It results in an increase in core loss which is reflected in the hysteresis loops as a form of the increase in loop area. At 600 Hz, the smaller area under the curve is due to the

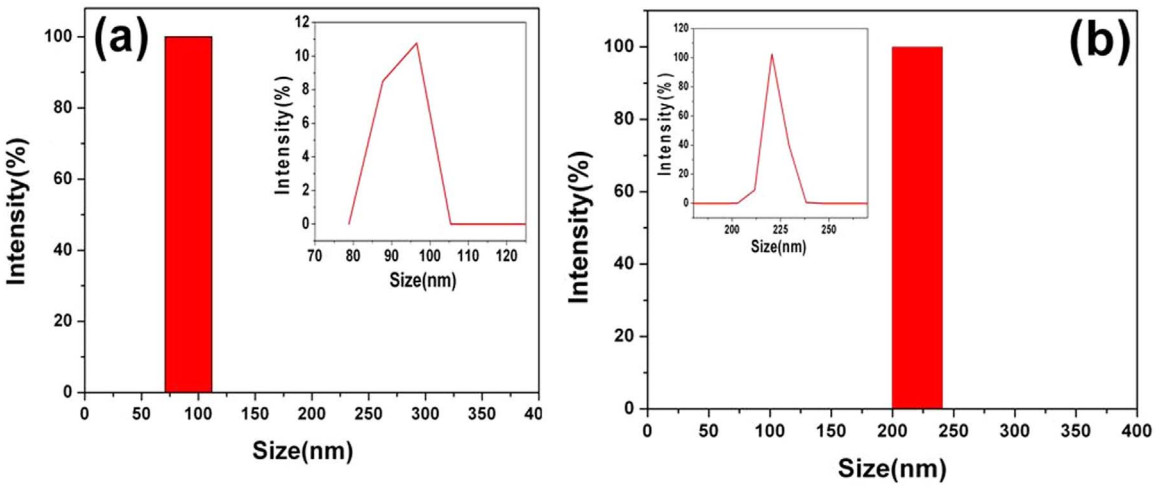

Fig. 6. Dynamic light scattering spectrum of (a) $CoFe_2O_4$ NPs in water, (b) folic acid coated $CoFe_2O_4$ NPs in water.

minor loop (applied field was not sufficient to saturate the sample at that frequency). The area under the curve of the hysteresis loops relates to the dissipation of energy as power loss during the magnetization process. This energy comes out as heat in cost of the AC hysteresis loss of the $CoFe_2O_4$ MNPs. This loss is a very crucial factor for their practical applications such as in microwave, radar technology and in hyperthermia treatment [18,28,29]. The dissipated energy in terms of power loss for the $CoFe_2O_4$ NPs has been calculated using the formula: Power Loss=(area inside the hysteresis loop × frequency of the applied AC field) and plotted against frequency in Fig. 3(l). It increases rapidly with increasing the frequency. A maximum power loss ~ 1 W/g has been obtained from this $CoFe_2O_4$ NPs which is reasonably sufficient for its applicability in hyperthermia. Here we can see that the power loss increases with increasing the applied AC field's frequency. Due to some limitation in our instrument we cannot go beyond the frequency of 1 kHz as high heating starts to affect the circuit of primary coil. But with this limitation we can conclude from the trend of the result that the advantage of this method is that heating effect can be controlled by changing the AC magnetic field frequency also. If we can modify the instrument and increase the frequency in MHz range we can have much higher loss power at very low applied field though with this limitation of instrument we can predict that our particles are highly efficient to produce much heat even at such low frequency.

Furthermore, we have tried to fit the frequency dependence of coercivity with an empirical formula $H_C \sim A \times f^n$, where A and 'n' are the parameters selected for the best fitting. The frequency dependent coercivity and its fitting have been plotted in Fig. 4. The above mentioned fitting function comes from the Gyorgy's proposed model to describe the dependence of coercivity on the applied field's frequency as given below [30]

$$H_C = \left(\frac{\pi f \beta x H_a}{M}\right)^n \quad (1)$$

where, f denotes the frequency of the applied AC field H_a. x, β and M are respectively the average domain wall width, the eddy current damping constant and the saturation magnetization. The model is completely structure independent and its frequency dependence arises from the eddy current damping in the material. According to this model, the exponent (n) should be ~0.5. In our fitting of the experimental results, the value of n is found to be 0.42 which is very close to the theoretical value as proposed by Gyorgy.

3.4. FT-IR study

To check the folic acid coating FT-IR study was done using KBr matrix method for the sample after folic acid coating. FT-IR graph is shown in Fig. 5. Here the peaks present at 576.05 and 418.55 cm^{-1} confirms the presence of the tetrahedral and octahedral site of cobalt ferrite which again confirms the phase of Co-ferrite and 1606.41, 1538.91, 1451.17, 1412.6, 1397.17, 1338.35, 1193.72, 1189.86, 1135.9, 1106.94, 1051.97, 839.84 cm^{-1} peaks are for folic acid [31–33] which confirms that the coating of folic acid on cobalt ferrite nano particle has been done here successfully.

3.5. Dynamic light scattering study

To investigate the size of the cobalt ferrite magnetic nanoparticle before and after coating with folic acid, the zeta sizer measurements were performed in water shown in Fig. 6(a and b). In Fig. 6(a) there was one peak appearing at 92.21 nm is quite higher than the size we got from TEM, may be due to agglomeration effect as the particles are highly ferromagnetic in character. Similarly when the nano particles were coated with folic acid, one peak appears at 222.42 nm represented in Fig. 6(b) explains a better attachment of folic acid with the cobalt ferrite nano particles and due to folic acid coating the size of the particle increases.

3.6. Loading efficiency of anticancer drug (DOX) to the particle

Drug loading efficiency for the particles was checked with the help of UV–vis absorption spectra taken for the Dox solution before (initial) and after (final) loading the drug into the particles, shown in Fig. 7. The absorption intensity was measured at 486 nm wavelength and it was observed that about 78% of drug was loaded, which was calculated using the Eq. (2) as given below.

$$\text{Dox loading efficiency} = \frac{(\text{Intensity}_{\text{Initial Dox solution}} - \text{Intensity}_{\text{Final Dox solution}})}{\text{Intensity}_{\text{Initial Dox solution}}} \times 100\ \% \quad (2)$$

3.7. Drug release experiments

After loading the particles with drug, they were undergone for drug release study at two different temperatures (i.e. 37 °C and 44 °C) with respect to time in PBS (pH=7.4) buffer solution. 10 mg of this drug (DOX) loaded particles were taken in 3 ml of PBS buffer solution and these experiments were carried out at 37 °C and 44 °C and the drug release intensity was measured at different interval of time with the help of UV–vis spectrometer. The representative graphs on relative drug release rate with time measured at two different temperatures are shown in Fig. 8. The graphs clearly show that the release efficiency is undoubtedly better at higher temperature probably due to the fact that at higher temperature the particles are heated up leading to detachment of drug molecules from the particles at faster rate. Fig. 8 depicts that within 6 h, 90% of the drug was released at 44 °C. Hence, we can conclude that the $CoFe_2O_4$ magnetic nano particle has potentiality to be used in temperature triggered drug release by hyperthermia therapy, where controlled release of drug in a noninvasive way is required.

4. Conclusion

We have successfully synthesized cubic shaped magnetic nano particles of cobalt ferrite. Structural characterization of these particles shows the pure phase of cobalt ferrite. Magnetic measurements offer about their suitability for the application of drug release using hyperthermia technique which can open new vistas in comparison to the conventional chemotherapy. Temperature dependent drug release studies give us new information about better treatment for cancer by controlled release in a non-invasive way. It also promises as a prudent tactic to overcome the drug delivery related problems when the problems of localization, toxicity, and cost are the main dominance. In a nutshell, we have successfully developed a drug delivery system to deliver the drug in a better way using hyperthermia technique under AC magnetic field.

Acknowledgements

One of the Authors Chaitali Dey would like to thank Centre of Excellence in Systems Biology & Biomedical Engineering, University College of Technology, for providing Research assistantship under CoE-TEQIP-II, University of Calcutta to carry out this work. Arup Ghosh is thankful to SERB, DST, Govt. of India for providing the financial support through National Post-Doctoral Fellowship (PDF/2015/000599). All the authors gratefully acknowledge Centre for Research in Nano science and Nanotechnology (CRNN) and S.N. Bose National centre for basic sciences for providing laboratory facilities. Authors are thankful to the Department of Science and Technology, Government of India for the funding under the project SR/WOS-A/CS-15/2013.

References

[1] V.T. DeVita, E. Chu, Cancer Res. 68 (2008) 8643–8653.
[2] O. Veiseh, J.W. Gunn, M. Zhang, Adv. Drug Deliv. Rev. 62 (2010) 284–304.
[3] V.V. Mody, A. Cox, S. Shah, A. Singh, W. Bevins, H. Parihar, Appl. Nanosci. 4 (2014) 385–392.
[4] B.A. Chabner, T.G. Roberts, Nat. Rev. Cancer 5 (2005) 65–72.
[5] G. Tiwari, R. Tiwari, B. Sriwastawa, L. Bhati, S. Pandey, P. Pandey, S.K. Bannerjee, Int. J. Pharm. Invest. 2 (2012) 2–11.
[6] P. Rathee, A.K, S. Sidhu, Curr. Nanomed. 6 (2016) 50–62.
[7] A.M. Alkilany, C.J. Murphy, J. Nanopart. Res. 12 (2010) 2313–2333.
[8] X.X.-H. Peng, X. Qian, H. Mao, A.A.Y. Wang, Z.G. Chen, S. Nie, D.M. Shin, Int. J. Nanomed. 3 (2008) 311–321.
[9] W.B. Liechty, D.R. Kryscio, B.V. Slaughter, N.A. Peppas, Annu. Rev. Chem. Biomol. Eng. 1 (2010) 149–173.
[10] D. Balogh, R. Tel-Vered, R. Freeman, I. Willner, J. Am. Chem. Soc. 133 (2011) 6533–6536.
[11] H. Chen, T. Moore, B. Qi, D.C. Colvin, E.K. Jelen, D.A. Hitchcock, J. He, O.T. Mefford, J.C. Gore, F. Alexis, J.N. Anker, ACS Nano 7 (2013) 1178–1187.
[12] G. Saito, J.A. Swanson, K.-D. Lee, Adv. Drug Deliv. Rev. 55 (2003) 199–215.
[13] K. Maaz, M. Usman, S. Karim, A. Mumtaz, S.K. Hasanain, M.F. Bertino, J. Appl. Phys. 105 (2009) 113917.
[14] D. Sarkar, M. Mandal, K. Mandal, J. Nanosci. Nanotechnol. 14 (2014) 2307–2316.
[15] L.H. Reddy, J.L. Arias, J. Nicolas, P. Couvreur, Chem. Rev. 112 (2012) 5818–5878.
[16] J.-C. Bacri, M. de Fatima Da Silva, R. Perzynski, J.-N. Pons, J. Roger, D. Sabolovic', A. Halbreich, U. Häfeli, W. Schütt, J. Teller, M. Zborowski (Eds.), Scientific and Clinical Applications of Magnetic Carriers, Springer US, Boston, MA, 1997, pp. 597–606.
[17] M. Kurian, S. Thankachan, D.S. Nair, E. K, B. Aswathy, A. Thomas, K.T.B. Krishna, J. Adv. Ceram. 4 (2015) 199.
[18] M.M. Goswami, C. Dey, A. Bandyopadhyay, D. Sarkar, M. Ahir, J. Magn. Magn. Mater. 417 (2016) 376–381.
[19] D. Sarkar, A. Ghosh, R. Rakshit, K. Mandal, J. Magn. Magn. Mater. 393 (2015) 192–198.
[20] M. Bañobre-López, A. Teijeiro, J. Rivas, Rep. Pract. Oncol. Radiother. 18 (2013) 397–400.
[21] C.F. Huang, X.Z. Lin, W.H. Lo, in: Proceedings of the 2010 Annu. Int. Conf. IEEE Eng. Med. Biol., 2010, pp. 3229–3232.
[22] R. Weissleder, M. Papisov, Rev. Magn. Reson. Med. 4 (1992) 1.
[23] L. Zhang, F.X. Gu, J.M. Chan, A.Z. Wang, R.S. Langer, O.C. Farokhzad, Clin. Pharmacol. Ther. 83 (2008) 761–769.
[24] C.F. Thorn, C. Oshiro, S. Marsh, T. Hernandez-Boussard, H. McLeod, T.E. Klein, R.B. Altman, Pharmacogenet. Genom. 21 (2011) 440–446.
[25] A. Monshi, World J. Nano Sci. Eng. 02 (2012) 154–160.
[26] R. Chen, M.G. Christiansen, P. Anikeeva, ACS Nano 7 (2013) 8990–9000.
[27] K. Maaz, A. Mumtaz, S.K. Hasanain, A. Ceylan, J. Magn. Magn. Mater. 308 (2007) 289–295.
[28] H. Wang, Z. Yuan, Z. Liu, T. Zhou, M. Zhang, K. Chan, in: Proceedings of the 2015 IEEE Magn. Conf., 2015, p. 1.
[29] J. Sun, W. Wang, Q. Yue, Materials 9 (2016) 231.
[30] C. Piotrowski, M. Yagi, T. Sawa, J. Appl. Phys. 69 (1991) 5337.
[31] R.B. Dhanakotti, V. Kaliyamoorthy, K.B. Mane Prabhu, S. Ravi, V. Radhakrishnan, M. Saminathan, A. Pandurangan, A. Mukannan, H. Yasuhiro, Int. J. Nanomed. 10 (2015) 189.
[32] C. Xiong, X. Yuan, J. Zhou, Y. Chen, F. Chen, L. Xu, *African J. Pharm. Pharmacol.* 7 (2013) 666–672.
[33] C.V. Durgadas, C.P. Sharma, K. Sreenivasan, Analyst 136 (2011) 933–940.